A novel Chk1/2–Lats2–14-3-3 signaling pathway regulates P-body formation in response to UV damage

Nobuhiro Okada[1], Norikazu Yabuta[1], Hirokazu Suzuki[1], Yael Aylon[2], Moshe Oren[2] and Hiroshi Nojima[1,*]

[1]Department of Molecular Genetics, Research Institute for MicroFbial Diseases, Osaka University, 3-1 Yamadaoka, Suita City, Osaka 565-0871, Japan
[2]Department of Molecular Cell Biology, The Weizmann Institute of Science, Rehovot 76100, Israel
*Author for correspondence (snj-0212@biken.osaka-u.ac.jp)

Accepted 9 September 2010
Journal of Cell Science 124, 57-67

doi:10.1242/jcs.072918

Summary

Proper response to DNA damage is essential for maintaining the integrity of the genome. Here we show that in response to ultraviolet (UV) radiation, the Lats2 tumor suppressor protein is phosphorylated predominantly by Chk1 and weakly by Chk2 at S408 in vivo, and that this process occurs at all stages of the cell cycle and leads to phosphorylation of 14-3-3γ on S59 by Lats2. Interaction of Lats2 and 14-3-3γ in vivo was confirmed by immunoprecipitation and western blot analysis. Phosphorylated 14-3-3γ translocates to the P-body, where mRNA degradation, translational repression and mRNA surveillance take place. Depletion of Lats2 or 14-3-3γ by siRNA inhibits P-body formation in response to UV, newly implicating Lats2 and 14-3-3 as regulators of P-body formation. By contrast, siRNA-mediated depletion of Lats1, a mammalian paralog of Lats2, showed no such effect. On the basis of these findings, we propose that the Chk1/2–Lats2–14-3-3 axis identified here plays an important role in connecting DNA damage signals to P-body assembly.

Key words: Chk1, DNA damage, 14-3-3, Lats/Warts, P-body

Introduction

The DNA damage response (DDR) is essential for maintaining the integrity of the genome, and DDR function is crucial for avoiding mutations leading to cancer or cell death. Failure of the DDR enhances genomic instability and facilitates the proliferation of pre-cancerous cells (Löbrich and Jeggo, 2007). The DDR functions through a DNA-damage signaling pathway that is regulated by DNA damage checkpoint proteins that respond to double-strand breaks, stalled replication forks and bulky lesions (Kastan and Bartek, 2004). Two major protein kinases, ataxia-telangiectasia muted (ATM) and ataxia-telangiectasia and Rad-3-related (ATR), and the downstream effector kinases Chk1 and Chk2, play a central role in the DNA damage checkpoint network (Bartek et al., 2007; Lavin, 2008; Cimprich and Cortez, 2008).

Lats2 (large tumor suppressor homolog 2) is one of the key regulators of the Hippo size control pathway, which is well conserved in vertebrates (Grusche et al., 2010; McNeill and Woodgett, 2010). Lats2 contributes not only to the stability of another key player in the Hippo pathway, YAP2 (yes-associated protein 2) transcription factor, through YAP2 phosphorylation, but also to the induction of p73 target genes involved in apoptosis, including those encoding p53AIP1, Bax, and PUMA (Strano et al., 2005; Kawahara et al., 2008). Lats2 knockout mice display embryonic lethality and MEFs from *Lats2*$^{-/-}$ mice have mitotic defects that include centrosome fragmentation and cytokinesis defects that result in nuclear enlargement and multinucleation (McPherson et al., 2004; Yabuta et al., 2007). Overexpression of Lats2 can induce G1–S arrest resulting from downregulation of cyclin E/CDK2 kinase activity (Li et al., 2003), G2–M arrest resulting from downregulation of cyclin B/Cdc2 kinase activity (Kamikubo et al., 2003), and apoptosis resulting from downregulation of expression of the anti-apoptotic proteins Bcl-2 and Bcl-$_X$L (Ke et al., 2004). Two oncogenic miRNAs, miR-372 and miR-373, directly inhibit the expression of Lats2, thereby allowing tumorigenic growth in the presence of p53 (Voorhoeve et al., 2006). Moreover, Lats2 acts in a newly described tumor suppressor axis, Lats2–Mdm2–p53, by interacting with Mdm2 to inhibit p53 ubiquitylation and promote p53 activation, which creates positive feedback preventing tetraploidization (Aylon et al., 2006). Fbw7, an E3 ubiquitin ligase, regulates the p53-dependent induction of Lats2 and p21 to prevent tetraploidization in response to microtubule poisons (Finkin et al., 2008). Furthermore, Lats2 also plays a role at an ATR–Chk1-mediated stress checkpoint in response to oncogenic H-Ras (Aylon et al., 2009). Thus, Lats2 plays a crucial role in the response to mitotic stress and DNA damage. However, much remains unknown about the molecular mechanisms by which Lats2 responds to these stresses.

MicroRNAs (miRNAs), endogenous RNAs of approximately 22 nucleotides, play an important role in the regulation of gene expression (Kim et al., 2009; Sharp, 2009). miRNAs are incorporated into miRNA-induced silencing complexes (miRISCs) including Argonaute (Ago) proteins and GW182, which can lead to either translational repression or decay of targeted mRNAs (Hutvagner and Simard, 2008; Carthew and Sontheimer, 2009). Ago2 localizes to cytoplasmic foci known as the processing bodies (P-bodies, also known as GW-bodies), which contain targeted mRNAs, miRNAs and GW182 (Liu et al., 2005). P-bodies are sites where untranslated mRNAs accumulate, and where mRNA degradation, translational repression, and mRNA surveillance take place (Eulalio et al., 2007; Franks and Lykke-Andersen, 2008). GW182 is a putative scaffold protein for P-body assembly, because siRNA-mediated depletion of GW182 disrupts P-body formation (Liu et al., 2005). The 14-3-3 proteins comprise a large and highly conserved family found in all eukaryotes; seven isoforms (β, γ, ε, η, σ, τ and ζ) have been identified in humans (Morrison, 2009). The 14-3-3 proteins bind to protein ligands that have been phosphorylated on serine/threonine residues at a consensus binding motif, RSxS(*P*)xP or Rx[Y/F]xS(*P*)xP, and thereby regulate

multiple cellular processes including enzyme activity, subcellular localization and protein–protein interactions (Morrison, 2009). Phosphorylation of 14-3-3 isoforms can also play an important regulatory role in various cellular events (Aitken, 2006).

In this report, we show that Lats2 is phosphorylated by Chk1 and Chk2 (Chk1/2) on serine 408 (S408) in response to UV damage; this promotes the phosphorylation of 14-3-3 by Lats2. The phosphorylated 14-3-3 translocates to the P-body and plays an important role in P-body formation. Thus, the Chk1/2–Lats2–14-3-3 axis identified here plays a novel role in the regulation of P-body formation, and is likely to affect translational repression.

Results

Lats2 is phosphorylated by Chk1 and Chk2 in vitro

Because Lats2 functions in response to mitotic toxins (Finkin et al., 2008), we surmised that Lats2 might also be regulated by DNA damage signals. To determine whether Lats2 is downstream of the DDR pathway, we first performed in vitro kinase assays to examine whether Lats2 is phosphorylated by Chk1 and Chk2, because Lats2 contains several consensus sequences for these protein kinases (supplementary material Fig. S1A,B). Because full-length Lats2 is very unstable, two truncated forms of glutathione-S-transferase (GST)-fused Lats2, Lats2N (amino acids 79–622) and Lats2Ckd (amino acids 622–1088), were used as substrates. Because there are no consensus sequences for Chk1 and Chk2 phosphorylation (RxxS) (O'Neill et al., 2002) at the N-terminal (1–78 amino acids) region of Lats2, we did not include it in the analysis. GST–Lats2Ckd, which has defective kinase activity due to the substitution of the catalytically essential lysine 697 residue with methionine, was used instead of intact Lats2C protein to prevent autophosphorylation of Lats2C. As shown in supplementary material Fig. S1B, GST–Chk2 efficiently phosphorylated GST–Lats2N in vitro. However, GST–Chk2 could not phosphorylate GST–Lats2Ckd. Next, to determine the site of Lats2 phosphorylation by Chk2, we performed in vitro kinase assays using a variety of deletion mutants and amino acid substitution mutants (supplementary material Fig. S1C–H). The results indicate that Chk2 phosphorylates Lats2 in vitro at four sites: S172, S380, S408 and S446 (Fig. 1A,B).

Next, we raised four phospho-specific antibodies specific for Lats2 S172, Lats2 S380, Lats2 S408 and Lats2 S446. Then, we performed an in vitro kinase assay with Chk1 as the kinase, and wild-type or mutated forms of Lats2 peptides (GST–Lats2$^{79\text{-}257}$-WT, GST–Lats2$^{79\text{-}257}$-S172A, GST–Lats2$^{347\text{-}561}$-WT, GST–Lats2$^{347\text{-}561}$-S380A, GST–Lats2$^{394\text{-}463}$-WT, GST–Lats2$^{394\text{-}463}$-S408A or GST–Lats2$^{394\text{-}463}$-S446A) as the substrate in the absence of [γ-^{32}P]ATP and performed western blot analysis using these phospho-specific antibodies (Fig. 1C–F). When the active form of Chk1 (Chk1-WT) was used, the phosphorylated forms of all wild-type Lats2 peptides were detected with the phospho-specific antibodies (Fig. 1C–F, lane 3). However, no phosphorylation was detected when the alanine-substitution mutants of the Lats2 peptides were used as substrates and a kinase-deficient Chk1 (Chk1-KD) was used as kinase.

Next, we performed a similar in vitro kinase assay for Chk2 (Fig. 1G–J). When wild-type Chk2 was used, the phosphorylated forms of all the wild-type Lats2 peptides were detected by the phospho-specific antibodies, as seen for Chk1 (Fig. 1G–J, lane 3). However, no phosphorylation

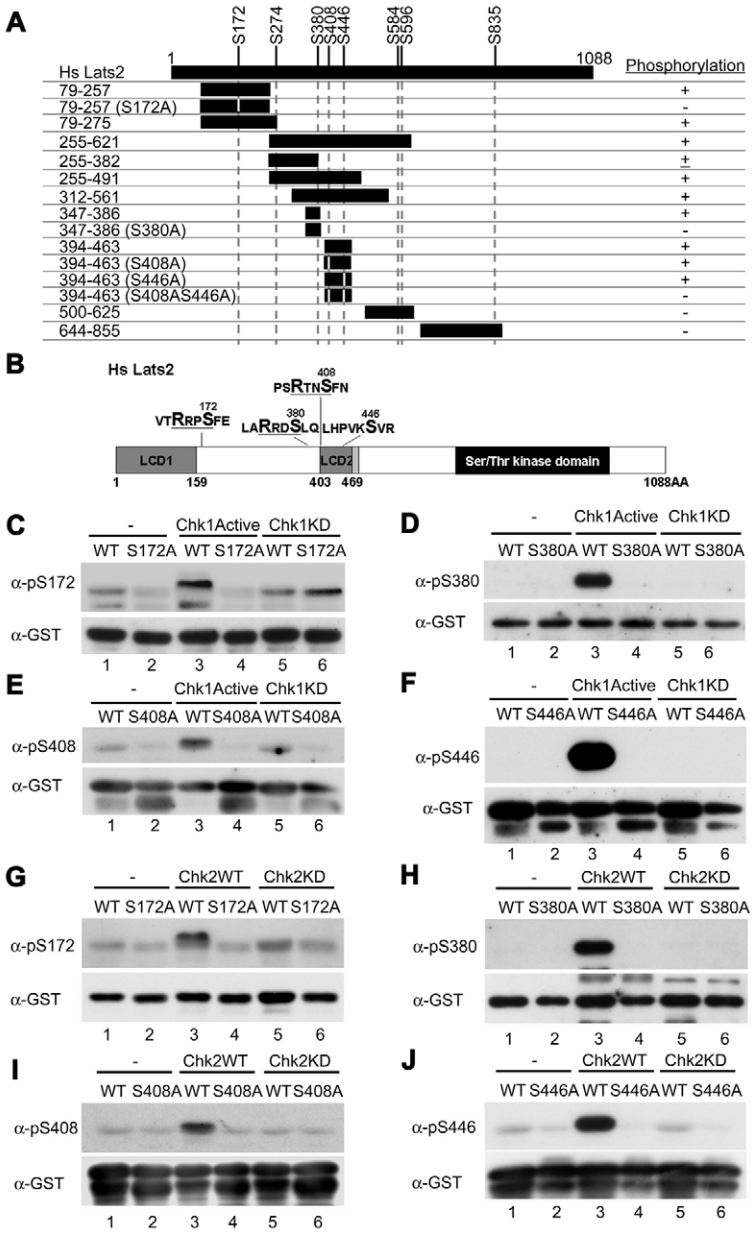

Fig. 1. Lats2 is phosphorylated by Chk1 and Chk2 in vitro. (**A**) Summary of our findings on Lats2 phosphorylation sites from in vitro kinase assays using a variety of deletion mutants. +, strong phosphorylation; ±, weak phosphorylation; –, no phosphorylation. (**B**) Lats2 sites phosphorylated by Chk2 and the consensus sequences for Chk1 and Chk2 phosphorylation (RxxS, underlined). LCD, Lats conserved domains. (**C–F**) In vitro kinase assays were performed using active GST–Chk1-WT or GST–Chk1-KD as the kinase, and GST–Lats2$^{79\text{-}257}$-WT, GST–Lats2$^{79\text{-}257}$–S172A (C), GST–Lats2$^{347\text{-}561}$-WT, GST–Lats2$^{347\text{-}561}$-S380A (D), GST–Lats2$^{394\text{-}463}$-WT, GST–Lats2$^{394\text{-}463}$-S408A (E) and GST–Lats2$^{394\text{-}463}$-S446A (F) as substrates. Western blot analyses were performed using anti-S172-*P*, anti-S380-*P*, anti-S408-*P*, and anti-S446-*P* antibodies, respectively. An anti-GST antibody was used as a loading control. (**G–J**) Western analyses were performed as for C–F using GST–Chk2-WT or GST–Chk2-KD as the kinase.

was detected when alanine-substitution mutants of the Lats2 peptides were used as substrates and kinase-deficient Chk2 was used as the kinase. Taken together, these results suggest that the phospho-specific antibodies specifically recognize the phosphorylated forms of S172, S380, S408 and S446, and that these Lats2 sites are phosphorylated by Chk1 and Chk2 in vitro.

Lats2-S408 is phosphorylated after UV irradiation in vivo

Previous studies have shown that Chk1 is activated by ATR through phosphorylation of the S317 and S345 residues in response to UV damage or the presence of a stalled replication fork, whereas Chk2 is activated by ATM through phosphorylation of T68 in response to double-strand breaks, although crosstalk exists between these pathways (Bartek and Lukas, 2003). To investigate whether Lats2 is phosphorylated in response to DNA damage in vivo, we irradiated U2OS cells containing intact p53 protein with UV light (50 J/m^2), performed western blot analysis using phospho-specific antibodies. We found weak and strong phosphorylation of S172 and S408, respectively, in response to the UV irradiation (data not shown).

To determine the detailed time course of Lats2 phosphorylation at S172 and S408, cell lysate from U2OS cells was incubated for between 5 and 480 minutes after UV irradiation, and then subjected to western blot analysis with anti-S172-*P* or anti-S408-*P* antibody (Fig. 2A). In U2OS cells, Lats2 phosphorylation at S408 was strongly detected between 30 and 120 minutes after UV irradiation. Subsequently, the intensity of the phosphorylated band decreased, presumably because of dephosphorylation. However, S172 phosphorylation was only weakly detected after UV irradiation. Similar results were obtained when we examined HeLa S3 cells (supplementary material Fig. S2A) in which *p53* was disrupted by the expression of human papillomavirus 18 viral protein E6 (Yee et al., 1985). Because these antibodies were not useful for immunoprecipitation and western analysis (data not shown), we cannot definitively dismiss the physiological significance of S172 phosphorylation, because the lack of signal does not necessarily indicate a lack of phosphorylation.

Next, to confirm that the bands detected by the anti-S408-*P* antibody resulted from Lats2 phosphorylation, cell lysate irradiated with UV for 8 hours was incubated with several concentrations of lambda protein phosphatase (PPase). The band detected by anti-S408-*P* disappeared after treatment with 200 U or 2000 U of PPase (supplementary material Fig. S2B, lanes 3, 4). As expected, the disappearance of these bands was completely blocked by the addition of phosphatase inhibitors after treatment with 2000 U of PPase (supplementary material Fig. S2B, lane 7). These results suggest that the bands detected by anti-S408 antibody were phosphorylated, and that their intensity depends on UV damage, and peaks between 30 and 120 minutes after UV irradiation.

To examine the roles of Chk1 and Chk2 in Lats2 phosphorylation on S408 after UV damage, we used short interfering RNA (siRNA) to deplete these kinases in U2OS cells (Fig. 2B). As expected, knockdown of Firefly luciferase (GL2), mouse transcription factor

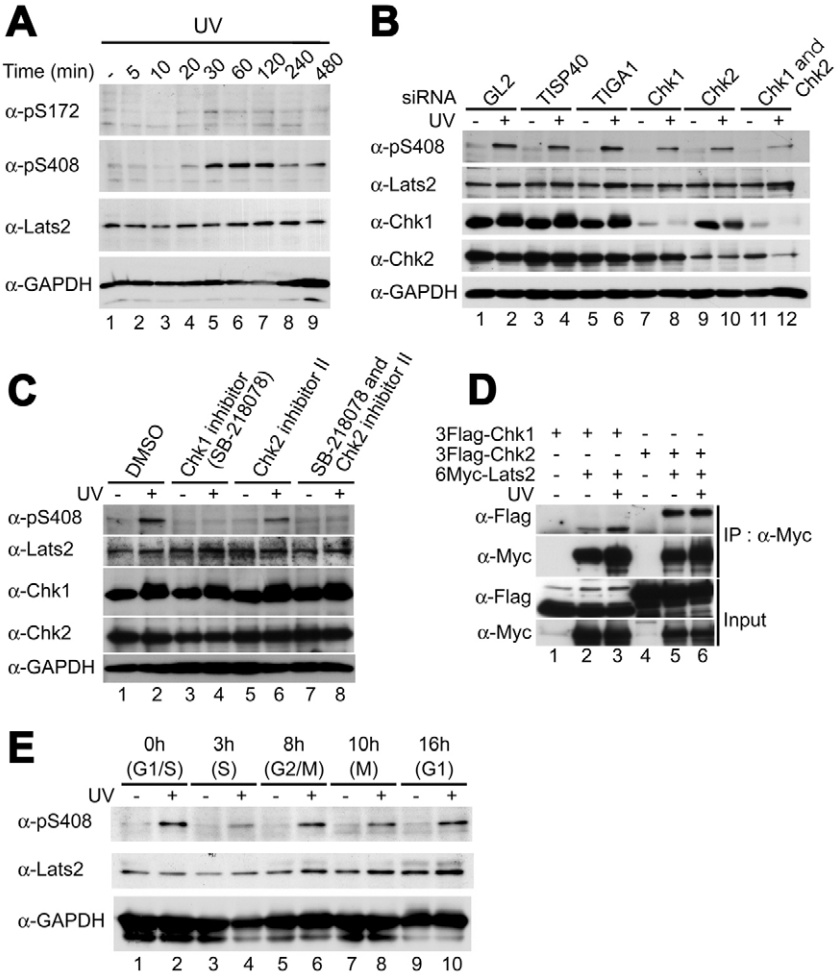

Fig. 2. Lats2 S408 is phosphorylated after UV irradiation in vivo. Western blot analyses were conducted using the indicated samples and antibodies. (**A**) The kinetics of Lats2 phosphorylation and dephosphorylation at S172 and S408 following exposure to UV irradiation (50 J/m^2) in U2OS cells. (**B**) U2OS cells were transfected with control siRNAs (targeting GL2, TISP40 and TIGA1), or with siRNAs specific for Chk1, Chk2, or both Chk1 and Chk2, irradiated UV (50 J/m^2), and incubated for 1 hour. (**C**) U2OS cells were treated with SB-218078 (1 μM), Chk2 inhibitor II (1 μM), or both SB-218078 and Chk2 inhibitor II for 24 hours before UV irradiation (50 J/m^2) for 1 hour. (**D**) Physical interaction of Lats2 with Chk1 and Chk2. 293T cells were co-transfected with vectors expressing 6Myc alone, 6Myc-tagged full length wild-type human Lats2 together with a vector expressing 3FLAG-tagged Chk1 and Chk2, as indicated. Total cell extracts and immunoprecipitates with anti-Myc antibody were separated by SDS-PAGE and then subjected to western blot analysis with anti-FLAG and anti-Myc antibodies. (**E**) U2OS cells were synchronized to the boundary of the G1–S phase using the thymidine–aphidicoline double block method and released after 0, 3, 8, 10 or 16 hours corresponding to the G1–S, S, G2–M, M, and G1 phases, respectively. UV irradiation was performed 1 hour before cell collection.

(TISP40), and human G0 specific gene (TIGA1), which are unrelated to DNA damage (Nagamori et al., 2005; Yabuta et al., 2006), served as negative controls and had no effect on S408 phosphorylation. By contrast, single knockdown of Chk1 or Chk2 modestly reduced phosphorylation. Double knockdown of both Chk1 and Chk2 reduced phosphorylation even more dramatically. To further investigate the roles of Chk1 and Chk2, we used two specific inhibitors, SB-218078 and Chk2 inhibitor II, to inhibit the kinase activities of Chk1 and Chk2, respectively (Fig. 2C). Treatment with DMSO served as a negative control and did not affect S408 phosphorylation. As expected, treatment with the Chk1 inhibitor SB-218078 completely abolished S408 phosphorylation (Fig. 2C, lane 4). By contrast, treatment with the Chk2 inhibitor II caused only a slight decrease in S408 phosphorylation (Fig. 2C, lane 6). Treatment with both reagents abolished S408 phosphorylation, which might be primarily due to the effects of SB-218078 (Fig. 2C, lane 8). These results suggest that Chk1, but not Chk2, plays a major role in S408 phosphorylation.

Then, we assessed and confirmed the in vivo interaction between Lats2 and Chk1/2 by immunoprecipitation and western blot analysis. As shown in Fig. 2D, Lats2 interacted with both Chk1 and Chk2. Interestingly, UV damage enhanced the interaction between Lats2 and Chk1, but did not enhance the interaction between Lats2 and Chk2. These results suggest that Lats2 S408 is phosphorylated by Chk1 and Chk2, in response to UV damage, and that Chk1 plays a predominant role in this process. Moreover, we examined whether S408 phosphorylation occurs throughout the cell cycle. U2OS cells were synchronized to G1–S, S, G2–M, M, or G1 using the thymidine–aphidicolin double block and release method; the synchronized cells were then UV irradiated and incubated for 1 hour before cell collection. S408 phosphorylation was detected at all stages of the cell cycle (Fig. 2E). Cell cycle synchronization was confirmed by FACS analysis (supplementary material Fig. S2C,D). Similar results were also obtained for HeLa S3 cells (supplementary material Fig. S2E–G).

Lats2 functions at the G1–S checkpoint and inhibits cell death

Because Lats2 is phosphorylated primarily by Chk1 in response to UV damage, we next investigated the role of Lats2 in regulation of the DNA damage checkpoint throughout the cell cycle. For this experiment, we used derivatives of U2OS cells in which endogenous Lats2 was stably knocked down by an integrated plasmid expressing Lats2-specific short hairpin RNA (shRNA), as described previously (Aylon et al., 2006). We first confirmed the Lats2 knockdown and subsequent reduction of the S408-*P* band by western blot analysis (Fig. 3A). Then, cell cycle progression in U2OS cells and in U2OS cells treated with control siRNA (U2OS/siControl) was examined using FACS analysis following UV irradiation, which confirmed that these cells were arrested at the G1–S checkpoint in response to UV damage (supplementary material Fig. S3A–D). This G1–S arrest in response to UV damage was consistent with another FACS analysis of the G1–S checkpoint (supplementary material Fig.

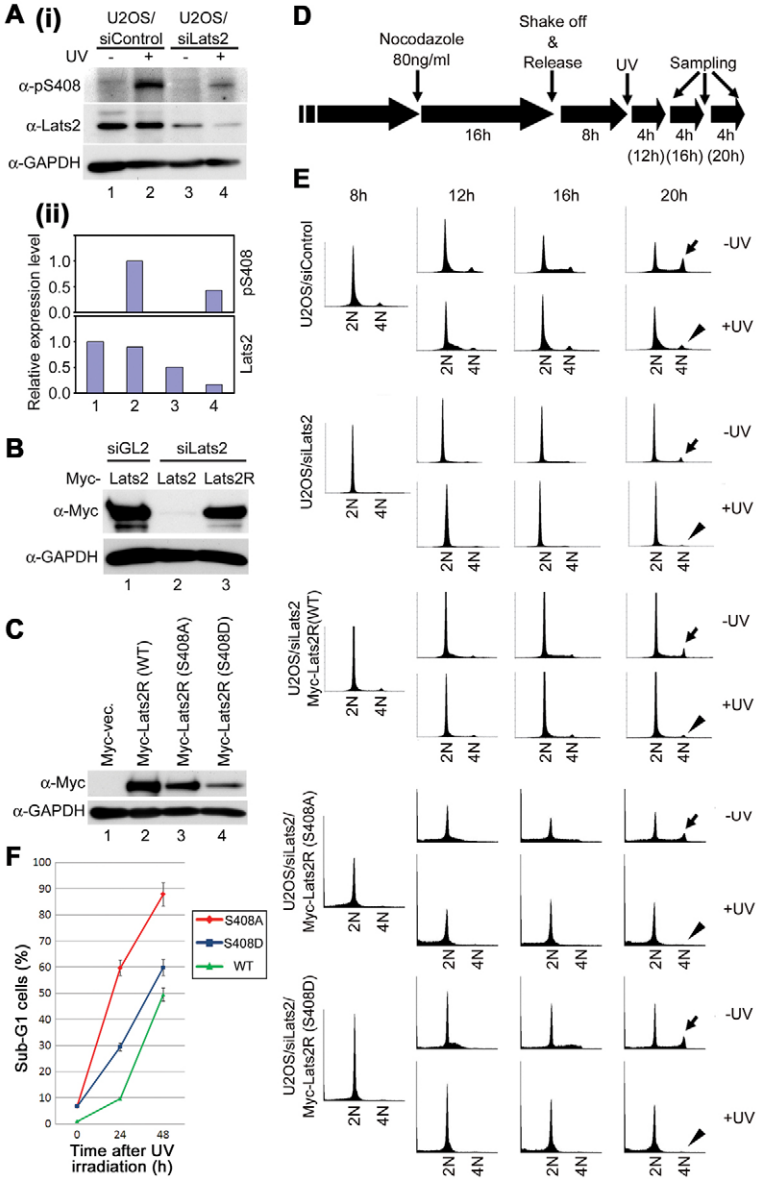

Fig. 3. Lats2 functions at the G1–S checkpoint in U2OS cells. (**A**) Confirmation of the successful knockdown of Lats2 in U2OS/siLats2 cells. (i) Western blot analyses were conducted using the indicated samples and antibodies. (ii) Bar graphs represent the intensity ratio of each band relative to the amount of GAPDH, a loading control. (**B**) Myc–Lats2R was not knocked down by siRNA targeting Lats2. U2OS cells were co-transfected with indicated DNA and siRNA in the indicated combinations. siGL2, siRNA targeting GL2. (**C**) Myc–Lats2R proteins are stably expressed in U2OS/siLats2 cells. (**D**) Experimental design for E. Cells were treated with nocodazol (80 ng/ml) for 16 hours. Then, the mitotic cells were collected by shake-off, transferred to new dishes, and incubated for 8 hours. Following this incubation, cells were irradiated with UV (50 J/m^2), and collected after the indicated periods of time. (**E**) FACS analysis of indicated cells monitoring cell cycle progression. 2N and 4N refer to diploid and tetraploid, respectively. Arrow or arrowheads indicates the G2–M peak before or after UV irradiation, respectively. (**F**) Frequency of sub-G1 cells in U2OS/siLats2/Myc–Lats2R(WT), U2OS/siLats2/Myc–Lats2R(S408A) and U2OS/siLats2/Myc–Lats2R(S408D) cells at 24 hours and 48 hours after UV irradiation. Means and standard deviations were obtained from three independent experiments.

S3E). By contrast, U2OS cells treated with siLats2-specific siRNA (U2OS/siLats2) were not arrested; the number of cells arrested at the G1–S checkpoint after UV irradiation decreased conspicuously from 40.9% (6 hours) to 27.3% (24 hours) compared with U2OS and U2OS/siControl cells (supplementary material Fig. S3A,B).

Next, we prepared mutants in which the phosphorylated serine residue was changed to a nonphosphorylatable alanine (S408A) or a phosphorylation-mimic aspartic acid (S408D). We also prepared RNA interference (RNAi)-refractory Lats2 (Lats2R) (Fig. 3B). We then generated U2OS/siLats2 strains that stably expressed Myc–Lats2R(WT), Myc–Lats2R(S408A), or Myc–Lats2R(S408D) (Fig. 3C). We used FACS analysis to study cell cycle progression in these stable cell lines after UV irradiation. Because we have shown that Lats2 functions at the G1–S checkpoint after UV damage (supplementary material Fig. S3A–D), these cells were irradiated with UV in the G1 phase and then analyzed. In these experiments, cells arrested in mitosis by treatment with nocodazole (80 ng/ml) for 16 hours were collected by shake-off, released for 8 hours and then UV irradiated (Fig. 3D). Indeed, all of these cells displayed decreased G2–M peaks after UV irradiation (Fig. 3E, compare arrows and arrowheads in the rightmost panels), which indicates that phosphorylation of Lats2 on S408 did not affect cell cycle progression through the G1–S checkpoint (Fig. 3E). By contrast, when these cells were analyzed by FACS at 24 and 48 hours after UV irradiation, a greater increase in the sub-G1 population was observed in U2OS/siLats2/Myc–Lats2R(S408A) cells than in U2OS/siLats2/Myc–Lats2R(S408D) or U2OS/siLats2/Myc–Lats2R(WT) cells (Fig. 3F).

Lats2 phosphorylates 14-3-3γ on S59

Because Lats2 is a serine/threonine kinase, we hypothesized that Lats2 functions as a mediator of DNA damage signals transmitted from Chk1 and Chk2 to the downstream targets. Activation of Lats2 kinase activity requires both the addition of Mob1A and phosphatase inhibition (Yabuta et al., 2007), and so the immunoprecipitate from 293T cells coexpressing GFP (green fluorescent protein)–Lats2 and 3FLAG–Mob1A was treated with okadaic acid during the kinase assays. Then, the immunoprecipitates were reacted with the candidate substrates, including Cdc14A, Cdc14B, p53, NPM, Cdh1, Hdm2 and 14-3-3γ, in the presence of [γ-^{32}P] ATP. We found that Lats2 phosphorylated 14-3-3γ conspicuously (Fig. 4A) better than all other candidates, which

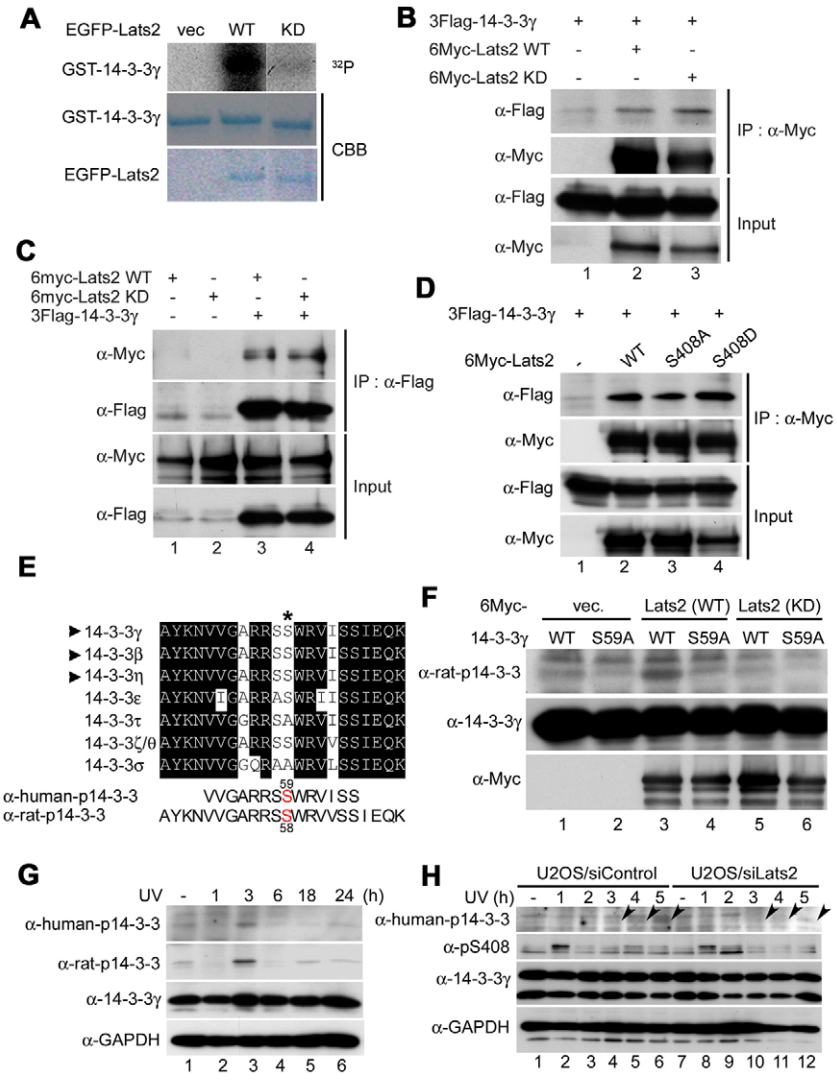

Fig. 4. 14-3-3γ phosphorylated at S59 by Lats2 in response to UV damage. Western blot analyses were conducted using the indicated samples and antibodies. (**A**) In vitro Lats2 kinase assay. (**B**) Physical interaction of Lats2 with 14-3-3γ. 293T cells were co-transfected with vectors expressing 6Myc alone, 6Myc-tagged full length wild-type human Lats2, or 6Myc-tagged full length kinase-deficient human Lats2 together with a vector expressing 3FLAG-tagged 14-3-3γ, as indicated. Total cell extracts and immunoprecipitates with anti-Myc antibody were separated by SDS-PAGE and then subjected to western blot analysis with anti-FLAG and anti-Myc antibodies. (**C**) Reciprocal immunoprecipitation and western analysis. Total cell extracts and immunoprecipitates with anti-FLAG antibody were separated by SDS-PAGE and then subjected to western blot analysis with anti-Myc and anti-FLAG antibodies. (**D**) Physical interaction of Lats2 with 14-3-3γ. 293T cells were co-transfected with vectors expressing 6Myc alone or 6Myc-tagged full length human Lats2 (wild-type, S408A or S408D), together with a vector expressing 3FLAG-tagged 14-3-3γ, as indicated. Total cell extracts and immunoprecipitates with anti-Myc antibody were separated by SDS-PAGE and then subjected to western blot analysis with anti-FLAG and anti-Myc antibodies. (**E**) Amino acid sequences of human 14-3-3 proteins surrounding the putative Lats2 phosphorylation site. An asterisk shows the S59 that is the site of phosphorylation by Lats2. Arrowheads show that 14-3-3 isoforms harbored the same amino acid sequence in the antigenic region. Residues that are conserved across at least six of seven isoforms are shown in black. (**F**) In vitro kinase assays were performed using 6Myc–Lats2 (WT or KD)-3FLAG–Mob1A immunoprecipitate as the kinase and 14-3-3γ (WT or S59A) as the substrate. (**G**) U2OS cells were exposed to UV irradiation and incubated for the indicated periods of time. Western blot analysis was performed using anti-human-phospho-14-3-3γ and anti-rat-phospho-14-3-3 antibodies. Anti-14-3-3γ and anti-GAPDH antibodies were used as loading controls. (**H**) U2OS/siControl and U2OS/siLats2 cells were exposed to UV irradiation and incubated for the indicated periods of time. Arrowheads indicate the western bands for phosphorylated 14-3-3 protein for comparison.

served as negative controls (supplementary material Fig. S4A–H). We also assessed and confirmed the in vivo interaction of Lats2 and 14-3-3γ by immunoprecipitation and western analysis. Specifically, the lysates from 293T cells co-transfected with 6Myc–Lats2 and 3FLAG–14-3-3γ were immunoprecipitated with anti-Myc (Fig. 4B) or anti-FLAG (Fig. 4C) antibodies and analyzed by western blotting. 3FLAG–14-3-3γ was detected in the 6Myc–Lats2 immune complex (Fig. 4B), and 6Myc–Lats2 was detected in the 3FLAG–14-3-3γ immune complex (Fig. 4C). Although 14-3-3γ binds to phosphorylated proteins, 3FLAG–14-3-3γ might not bind to phosphorylated Lats2 because none of the serine residues of Lats2 fit with the consensus binding motif of 14-3-3 proteins, RSxS(*P*)xP or Rx[Y/F]xS(*P*)xP (Aitken, 2006). Indeed, 3FLAG–14-3-3γ associated similarly to 6Myc–Lats2, regardless of whether S408 was intact (WT) or mutated (S408A or S408D). Namely, 3FLAG–14-3-3γ associates with 6Myc–Lats2 but its association is through the phosphorylated site(s) other than Lats2 S408 (Fig. 4D). These results suggest that 14-3-3γ is a phosphorylation substrate for Lats2.

To perform a detailed analysis of 14-3-3γ phosphorylation, we raised a phospho-specific antibody for 14-3-3γ(S59-*P*) (anti-human-phospho-14-3-3 antibody), because it has been speculated that the Lats kinase family phosphorylates substrates that contain an RxxS motif (Mah et al., 2005; Oka et al., 2008). We selected S59-*P* but not S64-*P* because14-3-3τ and 14-3-3σ contain alanine at this site (Fig. 4E), and thus their contributions can be excluded from our discussion. For comparison, we also purchased a commercially available phospho-specific antibody (anti-rat-phospho-14-3-3 antibody) that recognizes the same modification, S59 for human and S58 for rat 14-3-3 proteins, and whose immunogen peptide was longer than ours (Fig. 4E). Dot blot analysis revealed that anti-human-phospho-14-3-3 antibody specifically recognized phosphorylated forms, but not the unphosphorylated forms of this peptide (supplementary material Fig. S5A, upper panel). By contrast, anti-rat-phospho-14-3-3 antibody recognized the phosphorylated forms and also showed weak reactivity with the non-phosphorylated peptide (supplementary material Fig. S5A, arrowhead).

To determine whether Lats2 phosphorylates 14-3-3γ on S59, we performed a Lats2 kinase assay using purified 14-3-3γ in the absence of [γ-^{32}P] ATP followed by western blot analysis using the anti-rat-phospho-14-3-3 antibody. Indeed, we saw that wild-type Lats2 phosphorylated wild-type 14-3-3γ, but not 14-3-3γ(S59A), and that kinase-deficient Lats2 showed no phosphorylation (Fig. 4F). These results suggest that Lats2 phosphorylates 14-3-3γ on S59. Moreover, to investigate whether 14-3-3γ is phosphorylated in response to UV damage in vivo, U2OS cells irradiated with UV radiation were subjected to western blot analysis using the phospho-specific antibodies. As shown in Fig. 4G, 14-3-3γ phosphorylation was detected after 3 hours of UV irradiation. Furthermore, to examine whether Lats2 or Chk1/2 is responsible for the 14-3-3γ phosphorylation, we used U2OS/siControl and U2OS/siLats2 cells or performed siRNA-mediated Chk1/2 knockdown. Although control knockdown had no effect on 14-3-3γ phosphorylation, Lats2 or Chk1/2 knockdown significantly reduced phosphorylation (Fig. 4H, arrowhead; supplementary material Fig. S5B). We further found that Chk1/2 inhibition also significantly reduced phosphorylation (supplementary material Fig. S5C, arrowhead). These results suggest that 14-3-3γ is phosphorylated by Lats2 in response to UV damage, and this phosphorylation is regulated through the Chk1/2–Lats2 pathway. We next examined whether these antibodies could also recognize other 14-3-3 family members (14-3-3ε, 4-3-3τ and 4-3-3σ) by performing peptide dot blots. This analysis revealed that 14-3-3ζ/θ alone was weakly recognized by both antibodies (supplementary material Fig. S5D). Because 14-3-3γ, 4-3-3β and 4-3-3η harbor the same amino acid sequence in this antigenic region, the result indicates that they are the major phosphorylation substrates of Lats2. We next performed immunofluorescence analysis using these antibodies, and found that anti-human-phospho-14-3-3 antibody alone detected 14-3-3γ dots in the cytoplasm (Fig. 5A, left panels). These dots are not a background artifact because they disappeared after peptide competition and siRNA-mediated knockdown (supplementary material Fig. S6A).

14-3-3γ phosphorylated on S59 localizes to P-bodies

Candidate structures forming such cytoplasmic foci include the P-bodies, which are known to be involved in post-transcriptional regulation, including mRNA degradation, translational repression and mRNA surveillance (Eulalio et al., 2007; Jakymiw et al., 2007). Argonaute proteins, a key component of RNAi regulation, have been shown to localize to the P-body (Liu et al., 2005; Sen and Blau, 2005). We therefore examined whether phosphorylated 14-3-3γ colocalized with the P-body component Argonaute-2 (Ago2). Indeed, phosphorylated 14-3-3γ colocalized with Ago2 (Fig. 5A, upper panels). Furthermore, we followed the change in its localization after UV irradiation, because Lats2 was phosphorylated in response to UV damage (Fig. 5A, lower panels). Interestingly, the frequency of colocalized dots per cell (Fig. 5B) and the number of cells possessing at least one phosphorylated 14-3-3γ focus at the P-body (supplementary material Fig. S7A) markedly increased following UV irradiation (Fig. 5B). This result is consistent with a previous study showing that the concentrations of P-body components such as Dhh1p, the activator of decapping, and Dcp2, the decapping enzyme, were increased following UV exposure in yeast (Teixeira et al., 2005). Furthermore, to investigate whether only phosphorylated 14-3-3γ is localized to the P-body, we analyzed U2OS cells transiently expressing EGFP–14-3-3γ(S59D) or EGFP–14-3-3γ(S59A). We found that EGFP–14-3-3γ(S59D) but not EGFP–14-3-3γ(S59A) colocalized with the dot detected by anti-human-phospho-14-3-3 antibody (supplementary material Fig. S7C). Taken together, these results suggest that phosphorylated 14-3-3γ is a novel component of the P-body and that UV damage enhances its accumulation at the P-body.

We next performed siRNA-mediated depletion to examine the effects of Lats2 on appropriate localization of phosphorylated 14-3-3γ. We found that depletion of Lats2 abolished localization of phosphorylated 14-3-3γ to the P-body (Fig. 5C), whereas depletion of GL2, performed as a control, did not affect localization (Fig. 5D). Notably, the frequency of Ago2/14-3-3γ colocalized dots per cell (Fig. 5E) and the number of cells possessing at least one phosphorylated 14-3-3γ focus at the P-body (supplementary material Fig. S7C) both increased less in Lats2-depleted cells (Fig. 5E; supplementary material S7C) than in GL2-treated cells (Fig. 5F; supplementary material Fig. S7C) after UV damage.

14-3-3γ phosphorylated on S59 is required for P-body formation

It has been reported that Argonaute proteins localize not only to the P-body, but also to stress granules, upon exposure to stress stimuli (Leung et al., 2006). To confirm the P-body localization of 14-3-3γ(S59-*P*), we used another marker, GW182, which

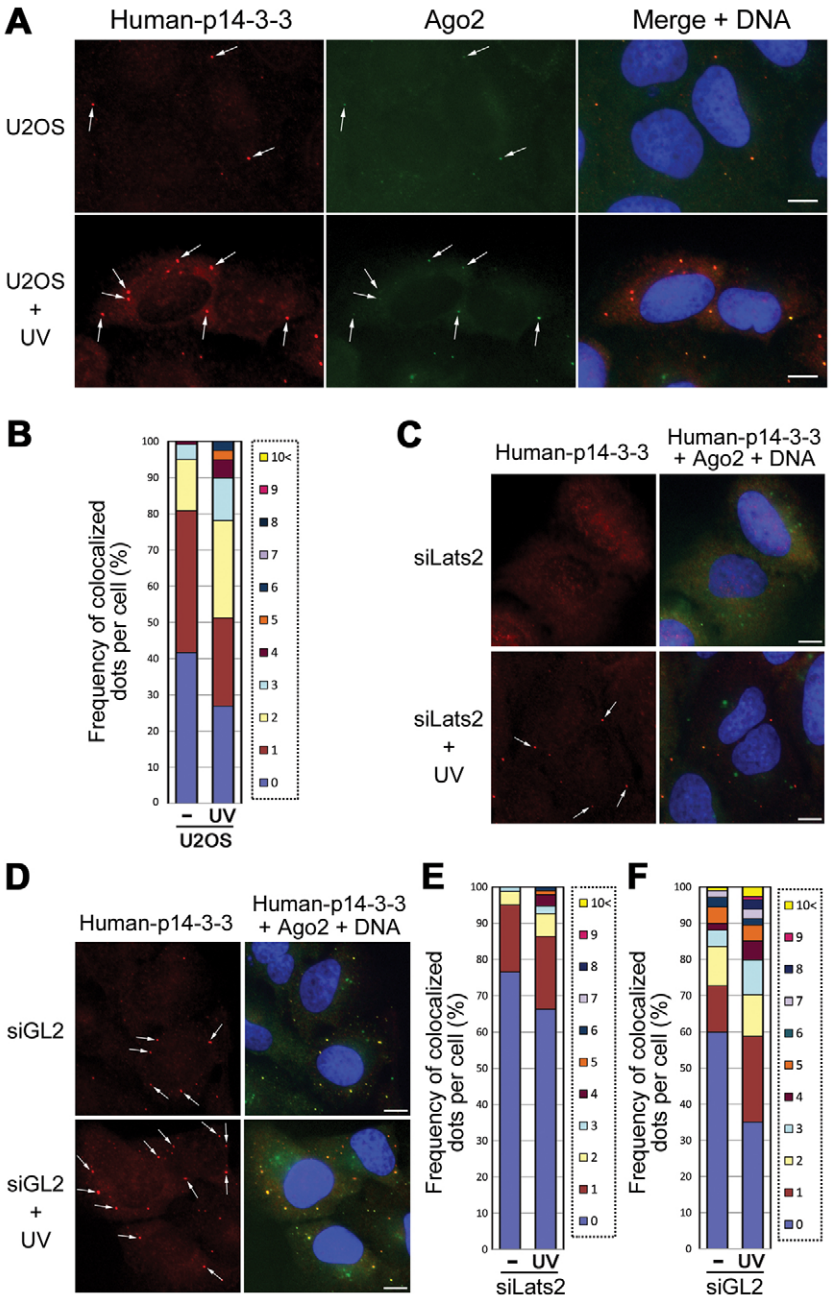

Fig. 5. 14-3-3γ phosphorylated at S59 by Lats2 localizes to the P-body. (**A**) U2OS cells were fixed with formaldehyde in the absence or presence of UV damage. S59-phosphorylated 14-3-3γ (red), the P-body (green) or DNA (blue) was visualized by anti-human-phospho-14-3-3 and anti-Ago2 antibodies or Hoechst 33258. White arrows point to colocalized dots. (**B**) Frequency of U2OS cells showing the indicated number of colocalized dots for human-phospho-14-3-3 and Ago2 (P-body marker) in the absence or presence of UV damage. (**C**,**D**) U2OS cells transfected with siRNA against Lats2 (siLats2) (C), or with GL2 (siGL2) as negative control (D), were fixed with formaldehyde in the absence or presence of UV damage and treated as for A. (**E**,**F**) Frequency of U2OS cells showing the indicated number of colocalized dots for human-phospho-14-3-3 and Ago2 in the absence or presence of UV damage. The graphs (B,E,F) show the average of three independent experiments. In each experiment, over 200 cells were counted. Scale bars: 10 μm.

specifically localizes to the P-body (Eulalio et al., 2007; Ding and Han, 2007). Indeed, we found that 14-3-3γ(S59-*P*) colocalizes with GW182 (Fig. 6A), and the frequency of colocalized dots per cell increased after UV irradiation (Fig. 6B). Furthermore, siRNA-mediated depletion of Lats2 abolished the localization of both phospho-14-3-3γ and GW182 to the P-body, whereas depletion of GL2 (a negative control) had no effect (Fig. 6C). Moreover, the frequency of colocalized dots (Fig. 6D) and the number of cells containing more than five P-bodies, as indicated by GW182 staining (supplementary material Fig. S7D), were considerably reduced, whereas the number of cells without P-bodies was conspicuously increased in Lats2-depleted cells compared with GL2-treated cells (supplementary material Fig. S7D). A similar dramatic reduction in the number of cells exhibiting phospho-14-3-3γ-stained P-body dots was observed in the Lats2-depleted cells (supplementary material Fig. S7E). These results suggest that phosphorylated 14-3-3γ can localize to P-bodies.

We then further examined the role of 14-3-3γ in the regulation of P-body formation, and found that siRNA-mediated depletion of 14-3-3γ decreased the localization of both phospho-14-3-3γ and GW182 to the P-body, whereas depletion of GL2 had no effect (Fig. 6E,F). We also examined the role of 14-3-3β, because the sequence of 14-3-3β is identical to that of 14-3-3γ in the phosphorylated region (Fig. 4E). As expected, deletion of 14-3-3β also decreased the localization of both phospho-14-3-3 and GW182 (supplementary material Fig. S6B–D). However, depletion of 14-3-3γ or 14-3-3β resulted in only a small decrease in localization compared with Lats2 depletion, suggesting that the two 14-3-3 isoforms cooperate in regulating P-body assembly. This is probably why the effect of siRNA targeting 14-3-3γ on GW182 positive foci

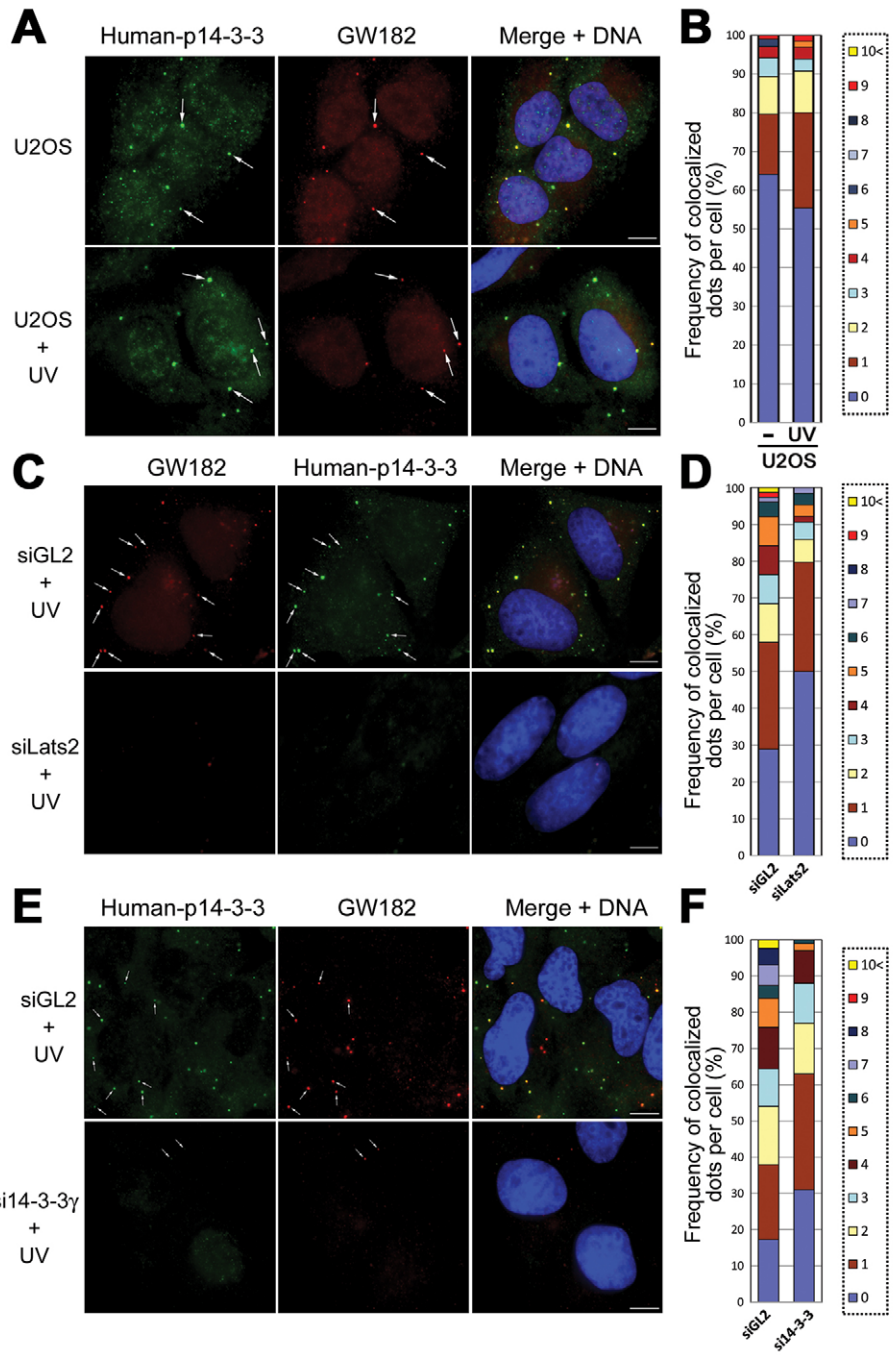

Fig. 6. 14-3-3γ phosphorylation at S59 is required for P-body formation. (**A**) U2OS cells were fixed with formaldehyde in the presence (upper panels) or absence (lower panels) of UV damage. (**C**,**E**) U2OS cells transfected with siRNA against Lats2 (siLats2) (C), 14-3-3γ (si14-3-3γ) (E), or GL2 (siGL2) (C,E) were fixed with formaldehyde after UV damage. S59-phosphorylated 14-3-3γ (green for A,E, red for C), GW182 (red for A,E, green for C) or DNA (blue) was visualized using anti-human-phospho-14-3-3 and anti-GW182 antibodies or Hoechst 33258. White arrows point to colocalized dots. (**B**,**D**,**F**) Frequency of U2OS cells showing the indicated number of colocalized dots for human-phospho-14-3-3 and GW182 in the absence or presence of UV damage, or after the indicated siRNA-mediated knockdown. The column graphs were drawn by averaging the data from three independent experiments. In each experiment, over 200 cells were counted unless otherwise indicated. Scale bars: 10 μm.

is not as drastic as that on 14-3-3γ positive foci (supplementary material Fig. S7F,G).

Next, we examined the effects of siRNA-mediated depletion of Lats1, a mammalian paralog of Lats2, and found that Lats1 depletion had no effect on P-body formation (supplementary material Fig. S8). We then examined the effects of Chk1 and Chk2 on P-body formation, and found that inhibition of Chk1 decreased the numbers of both 14-3-3(S59-*P*) and GW182 dots (Fig. 7). However, inhibition of Chk2 had no such effect. Taken together, these results demonstrate that the Chk1–Lats2–14-3-3 axis that we have identified here, but not Chk2 or Lats1, plays a crucial role in the formation of the P-body in response to UV-induced DNA damage.

Discussion

In the present study, we report that the Chk1–Lats2 axis acts as a phosphorylation cascade in response to UV damage. We demonstrate that Lats2 kinase is phosphorylated on S408 by the Chk1 and Chk2 kinases in response to UV irradiation, followed by Lats2 phosphorylation of 14-3-3γ on S59, which plays a key role in P-body formation and thus might influence translational repression (Fig. 7).

We have shown here that S408 of Lats2 is phosphorylated primarily by Chk1 and weakly by Chk2 in response to DNA damage both in vitro (Fig. 1) and in vivo (Fig. 2), which was confirmed by western blot analysis with phospho-specific antibodies. Our siRNA-mediated knockdown experiments (Fig.

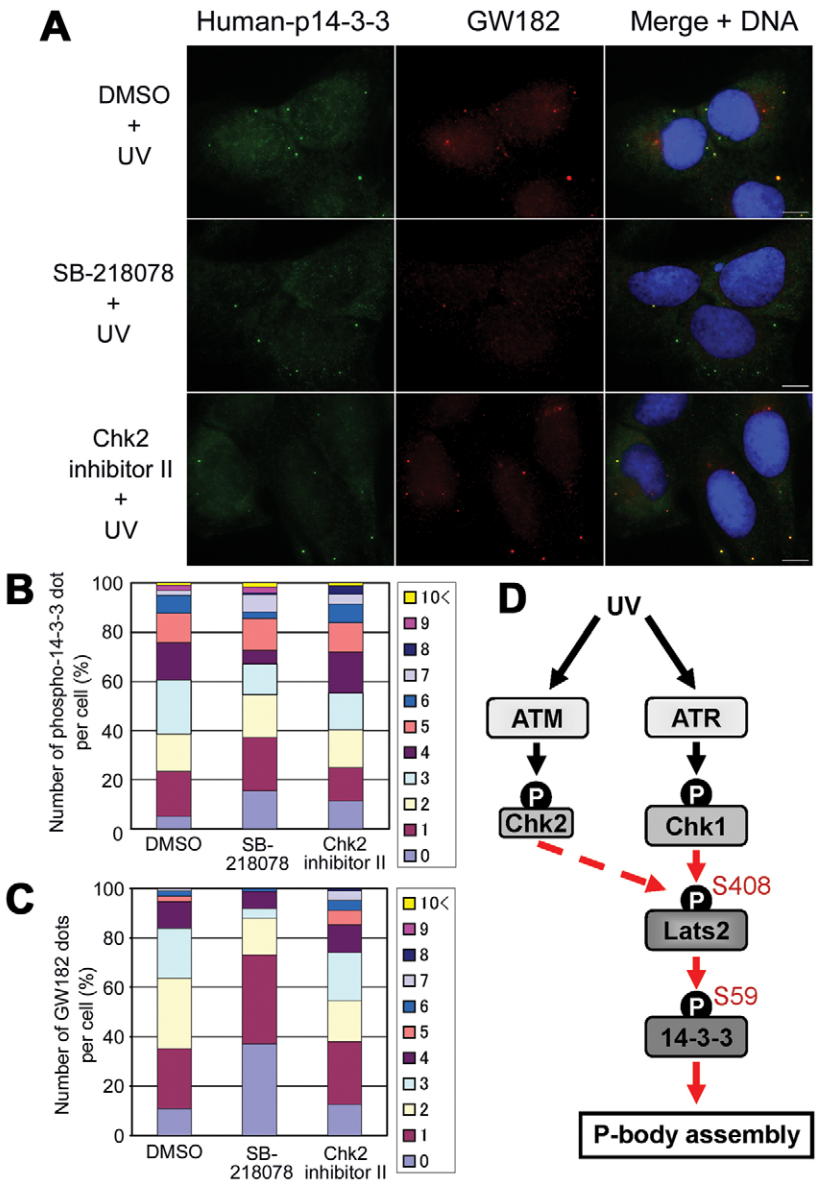

Fig. 7. Chk1 is required for P-body formation after UV damage. (**A**) U2OS cells treated with the Chk1 inhibitor SB-218078 or Chk2 inhibitor II were fixed with formaldehyde after UV damage and treated as for Fig. 6A. (**B**,**C**) Percentage of U2OS cells showing the indicated number of dots visualized with anti-14-3-3γ(S59-*P*) antibodies (B) or anti-GW182 (C). The column graphs were drawn by averaging three independent experiments. In each experiment, over 27 cells were counted. Scale bars: 10 µm. (**D**) Model summarizing the regulation of P-body formation following UV damage. Chk1 is activated by UV damage and induces Lats2 phosphorylation at S408. Activated Lats2 phosphorylates 14-3-3γ at S59, which promotes its translocation to the P-body and enhancement of P-body assembly. Red arrows indicate the pathway identified in this report.

2B) and inhibition experiments (Fig. 2C) revealed that Chk1 is mainly responsible for phosphorylation of Lats2 on S408, with Chk2 playing a supplementary role. Previous studies have shown that Lats2 is phosphorylated by Aurora-A and Mst2 (Toji et al., 2004). Here, we have shown that Chk1 and Chk2 are kinases targeting Lats2 as a phosphorylation substrate. Although phosphorylation of Lats2 on S408 did not affect cell cycle progression through the G1–S checkpoint, a larger increase in the sub-G1 population (cell death) was observed in Lats S408A mutant cells after UV irradiation (Fig. 3).

We also demonstrated here that Lats2 phosphorylates 14-3-3γ on S59 (Fig. 4), and that S59-phosphorylated 14-3-3γ formed cytoplasmic dots that colocalized with the P-body components Ago2 (Fig. 5) and GW182 (Fig. 6). Furthermore, Lats2 knockdown decreased the immunofluorescence signals of both 14-3-3 and GW182 in the P-body (Fig. 5 and Fig. 6). Previous studies have shown that depletion of GW182 by siRNA interferes with P-body assembly, and that P-body disruption induced by GW182 knockdown impairs miRNA-mediated gene silencing (Jakymiw et al., 2005; Liu et al., 2005). Consequently, it is thought that GW182 functions as a P-body scaffolding protein that provides a link between miRISC, mRNA and the proteins involved in translational repression and mRNA decay. On the basis of these results and reports, we propose here that 14-3-3 proteins, in particular 14-3-3γ, is a novel P-body component and is essential for P-body assembly, which might lead to translational repression (Fig. 7D).

In addition, Lats2-mediated phosphorylation of 14-3-3 proteins on S59 might play an important role in this regulation. GW182 is a phosphorylated protein (Eystathioy et al., 2002) and Ago2 is phosphorylated by MAPKAPK2 at S387 (Zeng et al., 2008); GW182 and Argonaute proteins have been shown to interact with each other (Ding and Han 2007; Liu et al., 2005). These reports support our proposed mechanism, because 14-3-3 proteins bind to phospho-proteins and regulate protein–protein interactions. miRNAs interact with mRNA targets with imperfect complementarity and repress the translation of target mRNA (Esquela-Kerscher and Slack, 2006). Thus, the interaction between miRNA and mRNA might be obscured. Therefore, we propose that miRNA expression, mRNA binding, and P-body assembly act cooperatively in regulating miRNA function. Notably, P-bodies are not required for general gene silencing (Eulalio et al., 2007), although this does not exclude the silencing of specific target genes under specific conditions. Thus, analysis of Lats2–14-3-3-mediated regulation of P-body assembly, including translational repression, will be the subject of future study by our group.

In summary, we conclude that the Chk1–Lats2–14-3-3 axis is crucial for the regulation of P-body assembly in response to DNA damage.

Materials and Methods

Generation of anti-phospho-specific antibodies

To generate five kinds of new polyclonal antibodies against the phosphorylated S172, S380, S408 and S446 sites in Lats2, and S59 in 14-3-3γ, rabbits were injected with the KLH-conjugated phospho-peptides CTRRPS(PO_3H_2)FEGTGDSFAS-YHQLSGT (S172-*P*), CATLARRDS(PO_3H_2)LQKPGLE (S380-*P*), CPSRT-NS(PO_3H_2)FNSHQ (S408-*P*), CLHPVKS(PO_3H_2)VRVLR (S446-*P*), and VVGARRSS(PO_3H_2)WRVISS (S59-*P*; 14-3-3γ). The antisera were then affinity-purified with a phospho-antigen peptide column. To eliminate nonspecific antibodies reacting with the unphosphorylated antigen peptide, the antibody preparation was passed through a non-phospho-peptide column (CTRRPSFEGTGDSFASYHQLSGT,

CATLARRDSLQKPGLE, CPSRTNSFNSHQ, CLHPVKSVRVLR or VVGARRSS-WRVISS).

Plasmid DNA constructs

cDNA encoding human Lats2-S408A and Lats2-S408D was amplified by PCR using pCMVmyc-full length human *LATS2* as a template with the primers shown in supplementary material Fig. S9. The PCR products were ligated into the *Pml*I sites of pCMVmyc-full length human *LATS2*. Human *LATS2R* cDNA was amplified by PCR using pCMVmyc-full length human *LATS2* as a template with primers shown in supplementary material Fig. S9. The PCR products were ligated into the *Hpa*I and *Xho*I sites of pCMVmyc-full length human *LATS2-WT*, *LATS2-S408A*, or *LATS2-S408D*. cDNA encoding human 14-3-3γ was amplified by PCR using a HeLa cDNA library and ligated into the *Asc*I and *Not*I sites of p3FLAG+*Asc*I, a modified version of p3×FLAG–CMV-7.1 (Sigma, St Louis, MO) containing the linker *Hin*dIII-*Asc*I-*Bmg*BI-*Not*I. All amplified sequences were confirmed by DNA sequencing.

Cell culture, transfection and cell synchronization

U2OS cells and 293T cells were maintained in Dulbecco's modified Eagle's medium (DMEM) supplemented with 10% fetal bovine serum (FBS; Hyclone Laboratory, UT), penicillin (100 U/ml) and streptomycin (100 μg/ml). HeLa S3 cells were maintained in DMEM supplemented with 5% FBS, penicillin (100 U/ml) and streptomycin (100 μg/ml). U2OS/siLats2 cells were maintained in DMEM supplemented with 10% FBS, penicillin (100 U/ml), streptomycin (100 μg/ml), and Blasticidin S (10 μg/ml; InvivoGen, San Diego, CA) to select for stably transfected clones (Aylon et al., 2006). U2OS/siLats2 cells were transfected with pCMVmyc vector, pCMVmyc–Lats2R(WT), pCMVmyc–Lats2R(S408A), and pCMVmyc–Lats2R(S408D) using the Lipofectamine and PLUS reagents, according to the manufacturer's instructions (Invitrogen, San Diego, CA). To generate stable clones, transfected cells were diluted and selected with G418 (800 μg/ml; Nacalai Tesque, Kyoto, Japan). Single colonies were isolated and validated for correct expression patterns. 293T and U2OS cells were transiently transfected with the indicated plasmids using the Lipofectamine and PLUS reagents according to the manufacturer's instructions. U2OS cells and HeLaS3 cells were synchronized to enter the G1–S phase using the thymidine–aphidicoline double block and release protocol. U2OS cells were collected at 0, 3, 8, 10 and 16 hours after release, corresponding to G1–S, S, G2–M, M and G1, respectively. HeLa S3 cells were collected at 0, 3, 6, 9 and 16 hours after release, corresponding to G1–S, S, G2–M, M, and G1, respectively. Cell synchrony was monitored by FACS analysis (BD Bioscience, San Jose, CA).

γ-ray irradiation

Cells were subjected to a 10-Gy dose of γ-radiation in a Gammacell 40 Exactor Research Irradiator (MDS Nordion, Ontario, Canada) with a ^{137}C source. For UV irradiation with a germinal lamp at a rate of 0.22 J/m^2/s, the culture medium and cell plate cover were first removed.

Antibodies and chemicals

LA-2 antibody was used as described previously for detection of Lats2 protein (Aylon et al., 2006; Yabuta et al., 2007). Anti-Chk1 monoclonal and anti-Chk2 monoclonal antibodies were purchased from Sigma-Aldrich (Milwaukee, WI); anti-14-3-3γ polyclonal antibody was purchased from Santa Cruz Biotechnology (Santa Cruz, CA); anti-Myc monoclonal, and anti-GST monoclonal antibodies were purchased from MBL (Nagoya, Japan); anti-AGO2 monoclonal antibody was purchased from WAKO (Osaka, Japan); anti-14-3-3 (S58-*P*) polyclonal, and anti-GW182 monoclonal antibodies were purchased from Abcam (Cambridge, UK); and anti-GAPDH monoclonal antibody was purchased from Fitzgerald Industries International (Concord, MA). SB-218078 and Chk2 inhibitor II were purchased from Calbiochem (La Jolla, CA).

In vitro kinase assays and immunoprecipitation

In vitro kinase assays were performed for the Chk1 and Chk2 kinases with 150 ng of active Chk1 (Upstate-Millipore, Bedford, MA) or 2 μg of GST-purified Chk2, and 2 μg of GST-purified substrate for 30 minutes at 30°C in Chk1/2 kinase buffer (20 mM Tris-HCl pH 7.4, 15 mM $MgCl_2$, 1 mM DTT, 1 mM NaF, 0.1 mM Na_3VO_4) containing 25 μM ATP. For in vitro kinase assays using Lats2, 293T cells were transfected with GFP–Lats2-WT, pCMVmyc–Lats2-WT or pCMVmyc–Lats2-KD and 3FLAG–Mob1A, and treated with the serine/threonine phosphatase inhibitor okadaic acid (0.1 μM) for 3 hours before harvesting the lysates. These cell extracts were immunoprecipitated and the immunoprecipitates were incubated for 30 minutes at 30°C in Lats2 kinase buffer (20 mM PIPES pH 6.8, 4 mM $MnCl_2$, 1 mM DTT, 1 mM NaF, 0.1 mM Na_3VO_4) containing 20 μM ATP and 10 μCi [γ-^{32}P] ATP. Protein lysates were prepared by incubating cells in TNE250 lysis buffer (10 mM Tris-HCl pH 8.0, 250 mM NaCl, 1 mM EDTA, 0.25% NP-40, 2 mM Benzamidine, 1 mM PMSF, 1 μg/ml aprotinin, 10 μg/ml leupeptin, 1 μg/ml pepstatine A, 1 mM NaF, 1 mM Na_3VO_4, 10 mM β-glycerophosphate and 0.1 μM okadaic acid) at 4°C for 30 minutes. After centrifugation, the cleared lysates were incubated with 2 μg of antibodies for 2 or 3 hours at 4°C, after which the immune complexes were harvested by the addition of 30 μl of 50% protein A-Sepharose (Amersham Pharmacia Biotech, Piscataway, NJ) and washed with NETN150 buffer (20 mM Tris-HCl pH 8.0, 150 mM NaCl, 1 mM EDTA, and 0.5% NP-40).

In vitro Lats2 kinase assay

293T cells were co-transfected with EGFP–Lats2-WT or EGFP–Lats2-KD together with 3FLAG–Mob1A and treated with okadaic acid. Immunoprecipitates obtained from the cell extracts using anti-GFP antibody were mixed with GST–14-3-3γ, incubated in kinase buffer containing [γ-^{32}P] ATP for 30 minutes at 30°C, and then the proteins were separated by SDS-PAGE.

Immunofluorescence staining

U2OS cells were plated on coverslips and fixed by sequential incubations with 4% formaldehyde in PBS without calcium and magnesium [PBS(–)], 0.1% Triton X-100 in PBS(–) and 0.05% Tween-20 in PBS(–), each for 10 minutes at room temperature. After being washed, cells were incubated with anti-Lats2(S408-*P*), anti-14-3-3γ(S59-*P*), anti-GW182 or anti-Ago2, followed by incubation with Alexa Fluor 488 and 594 (Molecular Probes, Eugene, OR) –conjugated anti-rabbit/mouse IgG in TBST (100 mM Tris-HCl pH 7.5, 150 mM NaCl, 0.05% Tween-20) containing 5% FBS. DNA was stained using Hoechst 33258 (Sigma) and cells were observed using a BX51 microscope (Olympus).

FACS analysis

Cells were stained using the CycleTEST PLUS DNA Reagent Kit (BD Bioscience), according to the manufacturer's instructions. Analysis was performed using a BD FACScalibur with CellQuest software.

Western blot analysis

Total cellular extracts and immunoprecipitates resolved by SDS-PAGE were transferred to nitrocellulose filters. Western blotting was performed in TBST containing 5% non-fat milk or 5% BSA. Immunoreactive protein bands were visualized by using Western Lightning Chemiluminescence Reagent Plus (Perkin-Elmer, San Jose, CA).

siRNA

For knockdown of human Lats2, Lats1, Chk1, Chk2, 14-3-3γ, GL2, TIGA1 and TISP40, siRNA duplexes specific to these genes were used. The sequences are shown in supplementary material Fig. S9. siRNA specific to human 14-3-3β was purchased from Santa Cruz Biotechnology. siRNAs were transfected into U2OS cells and HeLs S3 cells using Oligofectamine (Invitrogen), according to the manufacturer's instructions. The cells were collected or fixed at 48 hours after transfection.

We are greatly obliged to Shingo Toji and Katsuyuki Tamai (MBL Co. Ltd, Nagoya, Japan) for their technical assistance and for providing cDNA encoding Chk1 and Chk2. We also thank Toshiya Hosomi, Souichi Nishihara, Mayumi Sugimoto and Kazuki Sasaki (Osaka University) for their technical assistance, and Patrick Hughes for critically reading the manuscript. This work was supported in part by Innovation Plaza Osaka of the Japan Science and Technology Agency (JST), Grants-in-Aid for Scientific Research (S and B) to H.N., and by the Encouragement of Young Scientists to N.Y. from the Ministry of Education, Culture, Sports, Science and Technology of Japan.

Supplementary material available online at http://www.biken.osaka-u.ac.jp/lab/molgenet/Supplementary%20data-JCS-2010.pdf.

References

Aitken, A. (2006). 14-3-3 proteins: a historic overview. *Semin. Cancer Biol.* **16**, 162-172.

Aylon, Y., Michael, D., Shmueli, A., Yabuta, N., Nojima, H. and Oren, M. (2006). A positive feedback loop between the p53 and Lats2 tumor suppressors prevents tetraploidization. *Genes Dev.* **20**, 2687-2700.

Aylon, Y., Yabuta, N., Besserglick, H., Buganim, Y., Rotter, V., Nojima, H. and Oren, M. (2009). Silencing of the Lats2 tumor suppressor overrides a p53-dependent oncogenic stress checkpoint and enables mutant H-Ras-driven cell transformation. *Oncogene* **28**, 4469-4479.

Bartek, J. and Lukas, J. (2003). Chk1 and Chk2 kinases in checkpoint control and cancer. *Cancer Cell* **3**, 421-429.

Bartek, J., Bartkova, J. and Lukas, J. (2007). DNA damage signalling guards against activated oncogenes and tumour progression. *Oncogene* **26**, 7773-7779.

Carthew, R. W. and Sontheimer, E. J. (2009). Origins and mechanisms of miRNAs and siRNAs. *Cell* **136**, 642-655.

Cimprich, K. A. and Cortez, D. (2008). ATR: an essential regulator of genome integrity. *Nat. Rev. Mol. Cell Biol.* **9**, 16-27.

Ding, L. and Han, M. (2007). GW182 family proteins are crucial for microRNA-mediated gene silencing. *Trends Cell Biol.* **17**, 411-416.

Esquela-Kerscher, A. and Slack, F. J. (2006). Oncomirs – microRNAs with a role in cancer. *Nat. Rev. Cancer* **6**, 259-269.

Eulalio, A., Behm-Ansmant, I. and Izaurralde, E. (2007). P bodies: at the crossroads of post-transcriptional pathways. *Nat. Rev. Mol. Cell Biol.* **8**, 9-22.

Eystathioy, T., Chan, E. K., Tenenbaum, S. A., Keene, J. D., Griffith, K. and Fritzler, M. J. (2002). A phosphorylated cytoplasmic autoantigen, GW182, associates with a unique population of human mRNAs within novel cytoplasmic speckles. *Mol. Biol. Cell* **13**, 1338-1351.

Finkin, S., Aylon, Y., Anzi, S., Oren, M. and Shaulian, E. (2008). Fbw7 regulates the activity of endoreduplication mediators and the p53 pathway to prevent drug-induced polyploidy. *Oncogene* **27**, 4411-4421.
Franks, T. M. and Lykke-Andersen, J. (2008). The control of mRNA decapping and P-body formation. *Mol. Cell* **32**, 605-615.
Grusche, F. A., Richardson, H. E. and Harvey, K. F. (2010). Upstream regulation of the hippo size control pathway. *Curr. Biol.* **20**, R574-R582.
Hutvagner, G. and Simard, M. J. (2008). Argonaute proteins: key players in RNA silencing. *Nat. Rev. Mol. Cell Biol.* **9**, 22-32.
Jakymiw, A., Lian, S., Eystathioy, T., Li, S., Satoh, M., Hamel, J. C., Fritzler, M. J. and Chan, E. K. (2005). Disruption of GW bodies impairs mammalian RNA interference. *Nat. Cell Biol.* **7**, 1267-1274.
Jakymiw, A., Pauley, K. M., Li, S., Ikeda, K., Lian, S., Eystathioy, T., Satoh, M., Fritzler, M. J. and Chan, E. K. (2007). The role of GW/P-bodies in RNA processing and silencing. *J. Cell Sci*. **120**, 1317-1323.
Kamikubo, Y., Takaori-Kondo, A., Uchiyama, T. and Hori, T. (2003). Inhibition of cell growth by conditional expression of kpm, a human homologue of Drosophila warts/lats tumor suppressor. *J. Biol. Chem.* **278**, 17609-17614.
Kastan, M. B. and Bartek, J. (2004). Cell-cycle checkpoints and cancer. *Nature* **432**, 316-323.
Kawahara, M., Hori, T., Chonabayashi, K., Oka, T., Sudol, M. and Uchiyama, T. (2008). Kpm/Lats2 is linked to chemosensitivity of leukemic cells through the stabilization of p73. *Blood* **112**, 3856-3866.
Ke, H., Pei, J., Ni, Z., Xia, H., Qi, H., Woods, T., Kelekar, A. and Tao, W. (2004). Putative tumor suppressor Lats2 induces apoptosis through downregulation of Bcl-2 and Bcl-x(L). *Exp. Cell Res.* **298**, 329-338.
Kim, V. N., Han, J. and Siomi, M. C. (2009). Biogenesis of small RNAs in animals. *Nat. Rev. Mol. Cell Biol.* **10**, 126-139.
Lavin, M. F. (2008). Ataxia-telangiectasia: from a rare disorder to a paradigm for cell signalling and cancer. *Nat. Rev. Mol. Cell Biol.* **9**, 759-769.
Leung, A. K., Calabrese, J. M. and Sharp, P. A. (2006). Quantitative analysis of Argonaute protein reveals microRNA-dependent localization to stress granules. *Proc. Natl. Acad. Sci. USA* **103**, 8125-8130.
Li, Y., Pei, J., Xia, H., Ke, H., Wang, H. and Tao, W. (2003). Lats2, a putative tumor suppressor, inhibits G1/S transition. *Oncogene* **22**, 4398-4405.
Liu, J., Rivas, F. V., Wohlschlegel, J., Yates, J. R., 3rd, Parker, R. and Hannon, G. J. (2005). A role for the P-body component GW182 in microRNA function. *Nat. Cell Biol.* **7**, 1261-1266.
Löbrich, M. and Jeggo, P. A. (2007). The impact of a negligent G2/M checkpoint on genomic instability and cancer induction. *Nat. Rev. Cancer* **7**, 861-869.
Mah, A. S., Elia, A. E., Devgan, G., Ptacek, J., Schutkowski, M., Snyder, M., Yaffe, M. B. and Deshaies, R. J. (2005). Substrate specificity analysis of protein kinase complex Dbf2-Mob1 by peptide library and proteome array screening. *BMC Biochem.* **21**, 6-22.
McNeill, H. and Woodgett, J. R. (2010). When pathways collide: collaboration and connivance among signalling proteins in development. *Nat. Rev. Mol. Cell Biol.* **11**, 404-413.
McPherson, J. P., Tamblyn, L., Elia, A., Migon, E., Shehabeldin, A., Matysiak-Zablocki, E., Lemmers, B., Salmena, L., Hakem, A., Fish, J. et al. (2004). Lats2/Kpm is required for embryonic development, proliferation control and genomic integrity. *EMBO J.* **23**, 3677-3688.
Morrison, D. K. (2009). The 14-3-3 proteins: integrators of diverse signaling cues that impact cell fate and cancer development. *Trends Cell Biol.* **19**, 16-23.
Nagamori, I., Yabuta, N., Fujii, T., Tanaka, H., Yomogida, K., Nishimune, Y. and Nojima, H. (2005). Tisp40, a spermatid specific CREM-like transcription factor, functions through unfolded protein response element via Rip pathway. *Genes Cells* **10**, 75-94.
Oka, T., Mazack, V. and Sudol, M. (2008). Mst2 and Lats kinases regulate apoptotic function of Yes kinase-associated protein (YAP). *J. Biol. Chem.* **283**, 27534-27546.
O'Neill, T., Giarratani, L., Chen, P., Iyer, L., Lee, C. H., Bobiak, M., Kanai, F., Zhou, B. B., Chung, J. H. and Rathbun, G. A. (2002). Determination of substrate motifs for human Chk1 and hCds1/Chk2 by the oriented peptide library approach. *J. Biol. Chem.* **277**, 16102-16115.
Sen, G. L. and Blau, H. M. (2005). Argonaute 2/RISC resides in sites of mammalian mRNA decay known as cytoplasmic bodies. *Nat. Cell Biol.* **7**, 633-636.
Sharp, P. A. (2009). The centrality of RNA. *Cell* **136**, 577-580.
Strano, S., Monti, O., Pediconi, N., Baccarini, A., Fontemaggi, G., Lapi, E., Mantovani, F., Damalas, A., Citro, G., Sacchi, A. et al. (2005). The transcriptional coactivator Yes-associated protein drives p73 gene-target specificity in response to DNA Damage. *Mol. Cell* **18**, 447-459.
Teixeira, D., Sheth, U., Valencia-Sanchez, M. A., Brengues, M. and Parker, R. (2005). Processing bodies require RNA for assembly and contain nontranslating mRNAs. *RNA* **11**, 371-382.
Toji, S., Yabuta, N., Hosomi, T., Nishihara, S., Kobayashi, T., Suzuki, S., Tamai, K. and Nojima, H. (2004). The centrosomal protein Lats2 is a phosphorylation target of Aurora-A kinase. *Genes Cells* **9**, 383-397.
Voorhoeve, P. M., le Sage, C., Schrier, M., Gillis, A. J., Stoop, H., Nagel, R., Liu, Y. P., van Duijse, J., Drost, J., Griekspoor, A. et al. (2006). A genetic screen implicates miRNA-372 and miRNA-373 as oncogenes in testicular germ cell tumors. *Cell* **124**, 1169-1181.
Yabuta, N., Onda, H., Watanabe, M., Yoshioka, N., Nagamori, I., Funatsu, T., Toji, S., Tamai, K. and Nojima, H. (2006). Isolation and characterization of the *TIGA* genes, whose transcripts are induced by growth arrest. *Nuc. Acids Res.* **34**, 4878-4892.
Yabuta, N., Okada, N., Ito, A., Hosomi, T., Nishihara, S., Sasayama, Y., Fujimori, A., Okuzaki, D., Zhao, H., Ikawa, M. et al. (2007). Lats2 is an essential mitotic regulator required for the coordination of cell division. *J. Biol. Chem.* **282**, 19259-19271.
Yee, C., Krishnan-Hewlett, I., Baker, C. C., Schlegel, R. and Howley, P. M. (1985). Presence and expression of human papillomavirus sequences in human cervical carcinoma cell lines. *Am. J. Pathol.* **119**, 361-366.
Zeng, Y., Sankala, H., Zhang, X. and Graves, P. R. (2008). Phosphorylation of Argonaute 2 at serine-387 facilitates its localization to processing bodies. *Biochem. J.* **413**, 429-436.

Journal of Cell Science